Modeling and Analysis of Force-Closure Properties for the Flexible Space Manipulator During Docking and Capturing Process

Xiaolong Ma, Ning Li, Chongfeng Zhang, Meng Chen, Xuemei Ju, Song Wu, and Huaiwu Zou

Abstract To acquire the rapid numerical simulation iteration with sufficient precision for the space manipulator, and resolve the contradiction between the force-closure properties elimination and vibration suppression, a parametric modelling method for the flexible space manipulator system was proposed in this paper. Based on this method and by adopting the Adams software, a rigid-flexible dynamic model for the space manipulator applying in the space station was developed, which contained the cabin, adapter and end-effector. Especially, the flexibility of the manipulator was introduced by employing the modal superposition method. Also, the stiffnesses of the harmonic reducer and torque sensor were respected in order to simulate the flexibility of manipulator joints. Then a typical working task represented as shifting the load module by using the space manipulator was selected to analyze its dynamic behavior during the docking and capturing process. Results showed that the joint error could be reduced by the flexibility deformation of the space manipulator. And it was found the contact force and joint load were positively related with joints stiffness. In general, the modeling method and dynamic model proposed in this paper could provide a reference for the design and operation setting for the space manipulator.

Keywords Space manipulator · Dynamic behavior · Force-closure properties · Flexible

1   Introduction

As a crucial operation component of the space station, the space manipulator plays an important role in the on-orbit assembly, testing and maintenance [1]. As the typical

---

X. Ma · N. Li · C. Zhang (✉) · M. Chen · X. Ju · S. Wu · H. Zou
Shanghai Institute of Aerospace System Engineering, Shanghai, P. R. China
e-mail: zhcf008@139.com

Shanghai Key Laboratory of Spacecraft Mechanism, Shanghai, P. R. China

1755

basic operation, it requires sufficient precision in the docking and capturing process. Moreover, it is critical to maintain the force closure during motion [2]. However, multi-flexible body characteristic is presented by the space station due to its large cabin volume and inertia. Especially, the quality of the docking section is equivalent to that of the docked section for the space station, which could aggravate the flexibility. Also, the light mass, low stiffness and large length of the space manipulator result to obvious flexibility. The end location error can be caused due to these high rigid-flexible coupling characteristics and it could lead to the force-closure phenomenon, which could bring about heavy load and enlarge the operating error of the space manipulator. Therefore, it is significant to investigate the force-closure properties for the flexible space manipulator during docking and capturing process.

A lot of research works have been done on the dynamic analysis of manipulators. In terms of modelling for the space manipulator, Guo et al. [3] have developed a space robot model by using the ADAMS software to study the dynamic behavior and the control strategy when capturing the target. Practically, it is vital to build a parametric modelling method for obtaining the precious dynamic behaviors of flexible space manipulator. It has been demonstrated that the attached institutions could affect the dynamic behavior of the manipulator [4]. In this regard, dynamic models of the whole system including the manipulator and base institutions have been developed by many researchers [5–7]. However, it should be noted the dynamic modelling and coupling effect of the manipulator are complicated when the flexibility and space working conditions are introduced. Recently, Du et al. [8] presented a flexible space robot dynamic model by the ADAMS software. In this model, the flexible panels, the joints angle and the central rigid body mass on the dynamic coupling were considered. Besides, a system model including the space manipulator and the target spacecraft was established by Kang [9] in order to evaluate the performance of the capture strategy. Especially, Sun [10] built a flexible manipulator dynamic model considering multiple clearance joints and the Young's moduli, which was more reliable compared with traditional model. And it was reported that the dynamic behaviors and kinematic precision was affected serious by the flexibility of the components, especially by the number of clearance joints. As a matter of fact, the force closure is responsible to the works accomplished of the space manipulator. Therefore, Monforte et al. [1] have tried to adopt a reinforcement learning algorithm to estimate the grasping configuration. The force closure principle was applied in the policy reward to make a quality index explored the surrounding space. Besides, Liu et al. [11] proposed a grasping algorithm of static analysis and force closure for human manipulator applied in the complexity of the unstructured environment. In their research, the force closure condition was simplified by assuming each contact forces were within the corresponding friction. Furthermore, Li et al. [12] investigated the influence of parameter uncertainty on its kinematic accuracy and dynamic behaviors of space deployable mechanisms for a two-link rigid manipulator. On account of maintaining force closure during motion for space robotics, Carabis and John [13] proposed a squeeze force adjusting approach, which was designed in a micro-gravity environment. Bo et al. [14] built a force-closure condition equation and compute the force-closure workspace for cable-driven parallel manipulators,

which had a high computational efficiency according the experimental results. Similarly, a new computation method for the force-closure workspace of manipulators was reported by Shinde [15].

As mentioned above, dynamic analysis and force-closure properties analysis have been conducted by many researchers. However, these researches focused on the simplified dynamic models and ignored the complex attached institutions. Especially, there is relatively literatures referred to the modelling of the rigid-flexible dynamic analysis of manipulator considering real working conditions and the whole system. In this paper, a kinematic structure analysis of the space manipulator with 7 degree of freedom (DOF) was firstly presented. Then, a parametric dynamic model including the flexible space manipulator and the space station was developed. Following, based on the proposed model, the dynamic behavior and force-closure properties of the space manipulator were investigated.

2 Kinematic Structure Analysis of the 7-DOF Space Manipulator

The space manipulator depicted in this paper is employed for the fine operations in the experimental cabin of the space station. In order to enhance the self-motion capability, a S-R-S (spherical-rotational-spherical) kinematic structure is adopted, which is similar to the anatomical structure of human arm. As Fig. 1 shows, it can be seen the space manipulator is six meters long and adds a twist joint between the second joint and third joint compared to the traditional 6-DOF manipulators. In fact, the twist joint is key to enable the self-motion capability of the space manipulator.

The standard Denavit-Hartenberg method (SDH) is adopted to build the link coordinate system as Fig. 2 shows. Meanwhile, the transformation matrix from frame {i − 1} to frame {i} can be computed from the corresponding SDH parameters table, which is depicted in Table 2. Notably, θ_i is the initial value of the ith joint, $i = 1$, 2,…,7 (Table 1).
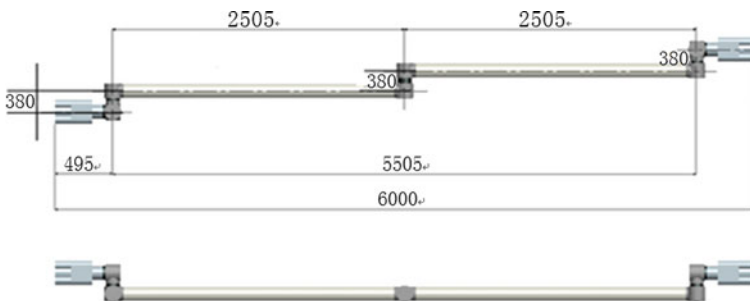

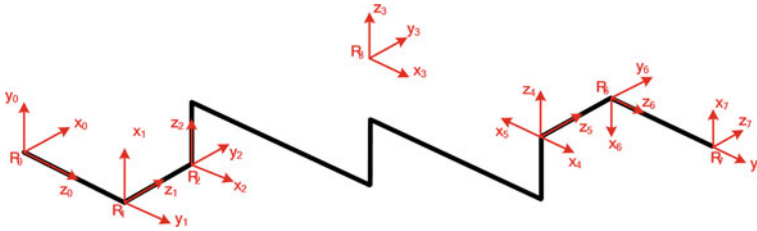**Fig. 1** The structure of S-R-S space manipulator

Fig. 2 The D-H model of the 7-DOF space manipulator

Table 1 SDH parameters of the 7-DOF space manipulator

i	θ_i	α_i	A_i (mm)	D_i (mm)
1	$\theta_1(90°)$	90°	0	650
2	$\theta_2(90°)$	90°	0	300
3	$\theta_3(0°)$	0	2300	900
4	$\theta_4(0°)$	0	2300	0
5	$\theta_5(180°)$	90°	0	0
6	$\theta_6(-90°)$	90°	0	300
7	$\theta_7(180°)$	90°	0	650

Table 2 Angular displacement planning of joints

Path	θ_2	θ_3	θ_4	θ_5	θ_6	θ_7
mb1–mb2	0.208	1.454	− 1.082	2.626	0.432	− 2.139
mb2–mb3	− 0.023	0.035	− 0.038	0.004	− 0.022	0.003

In order to solve the inverse kinematics problem, a reference plane of the manipulator should be determined firstly as referred in Ref. [16]. In this paper, the first joint θ_1 is fixed at 90°, which is known in the practical application. According to the SDH parameters, the given homogeneous pose of the manipulator in task space of the manipulator can be derived as:

$$
{}^1T_7 = A_2A_3A_4A_5A_6A_7 = \begin{bmatrix} n_x & s_x & a_x & p_x \\ n_y & s_y & a_y & p_y \\ n_z & s_z & a_z & p_z \\ 0 & 0 & 0 & 1 \end{bmatrix} \tag{1}
$$

where,

$$
{}^1R_7 = \begin{bmatrix} n_x & s_x & a_x \\ n_y & s_y & a_y \\ n_z & s_z & a_z \end{bmatrix} \tag{2a}
$$

$$^1P_7 = \begin{bmatrix} p_x & p_y & p_z \end{bmatrix}' \tag{2b}$$

where, $^1R_7$ and $^1P_7$ denotes the rotation and translation component of the manipulator pose relative to the base, respectively. A_i represents the homogeneous transformation from one assigned reference link (i) relative to the previous link ($i - 1$).

Based on Eqs. (1) and (2), using the relation between one assigned reference link (i) relative to the previous link ($i - 1$), θ_2 can be obtained as:

$$\theta_2 = a \tan 2\left(\frac{a}{b}\right) + a \tan 2\left(\frac{\pm\sqrt{a^2 + b^2 - d_3^2}}{d_3}\right) \tag{3}$$

where,

$$\begin{aligned} a &= p_x n_x + p_y n_y + p_z n_z - d_1 n_z \\ b &= -(p_x a_x + p_y a_y + p_z a_z + d_1 a_z) \end{aligned} \tag{4}$$

Similarly, the values of other joints can be given by:

$$\theta_6 = a \cos(-s_x s_2 + s_y c_2) \quad \text{or} \quad 2\pi - a \cos(-s_x s_2 + s_y c_2) \tag{5a}$$

$$\theta_7 = a \tan 2\left(\frac{(a_x s_2 - a_y c_2) \sin \theta_6}{(n_x s_2 - n_y c_2) \sin \theta_6}\right) \tag{5b}$$

$$\theta_4 = a \cos\left(\frac{B_1^2 + B_2^2 - a_4^2 - a_3^2}{2a_4 a_3}\right) \text{ or } 2\pi - a \cos\left(\frac{B_1^2 + B_2^2 - a_4^2 - a_3^2}{2a_4 a_3}\right) \tag{5c}$$

$$\theta_3 = a \tan 2\left(\frac{(a_4 c_4 + a_3) B_2 - (a_4 s_4) B_1}{(a_4 c_4 + a_3) B_1 + (a_4 s_4) B_2}\right) \tag{5d}$$

$$\theta_5 = a \tan 2\left(\frac{(c_2 n_x + s_2 n_y) s_7 - (c_2 a_x + s_2 a_y) c_7}{-s_7 n_z + c_7 a_z}\right) - \theta_3 - \theta_4 \tag{5e}$$

where, s_i denotes $\sin(\theta_i)$, c_i denotes $\cos(\theta_i)$, and

$$\begin{aligned} B_1 &= -((c_2 n_x + s_2 n_y) s_7 - (c_2 a_x + s_2 a_y) c_7) d_6 - (c_2 s_x + s_2 s_y) d_7 + c_2 p_x + s_2 p_y \\ B_2 &= -(s_7 n_z - c_7 a_z) d_6 - s_z d_7 + p_z - d_2 \end{aligned} \tag{6}$$

So far, 8 groups of inverse solutions have been obtained and the kinematic analysis of the space manipulator has been fulfilled and the power-minimizing principle is adopted to select the optimal solution. Following that, the inverse kinematic solutions could be employed to obtain the end pose of the space manipulator in the dynamic simulation.

3   Dynamic Model of the Space Manipulator System

Firstly, the joint model is built as Fig. 3 shows. The motor drives the gear 1 through the reduction ratio and drives the gear 2 through the meshing force. Besides, the torsion spring is adopted to simulate the joint flexibility, whose stiffness is consisted of harmonic reducer stiffness and torque sensor stiffness in series. Moreover, the joint damping is mainly composed of harmonic reducer damping and torque sensor damping.

1. Shell 2. Torque Sensor 3. Torque Sensor PCB 4. Panel 5. Driving Circuit Board 6. Brake 7. Motor 8. Harmonic Reducer 9. Transformer

The flexibility of arm link has a great effect on the flexibility of the space manipulator. In this paper, the modal superposition method is applied to simulate the flexibility. Namely, the finite element model of the arm link is established with one end fixed and the other end free and computed by ABAQUS Software. Also, the sweep function is selected as the meshed strategy. The modal analysis of the arm link is conducted in order to obtain first 14 modes. Then the modal neutral file can be acquired and used in the co-simulation process.

The end effector model is built as Fig. 4 shows, which is installed between the shoulder and wrist of the arm link. The motor drives the worm shaft through the reducer and transfer the movement to the mobile platform. With the moving control

Fig. 3 Dynamic model of joint **a** overall schematic **b** detailed structure
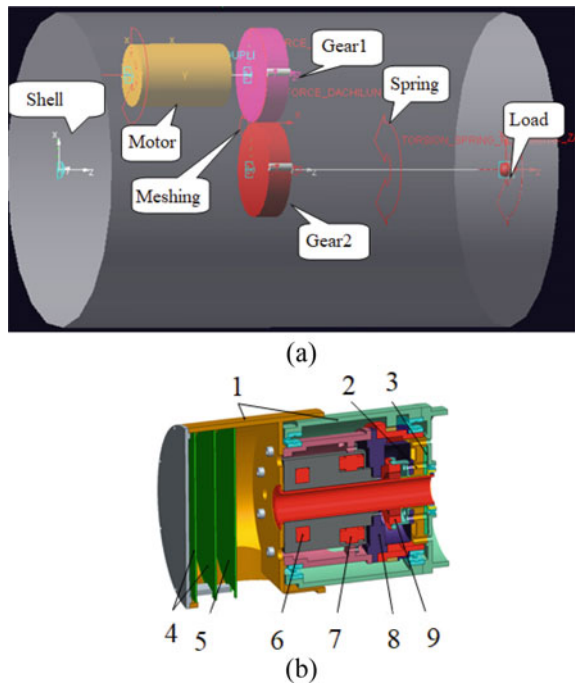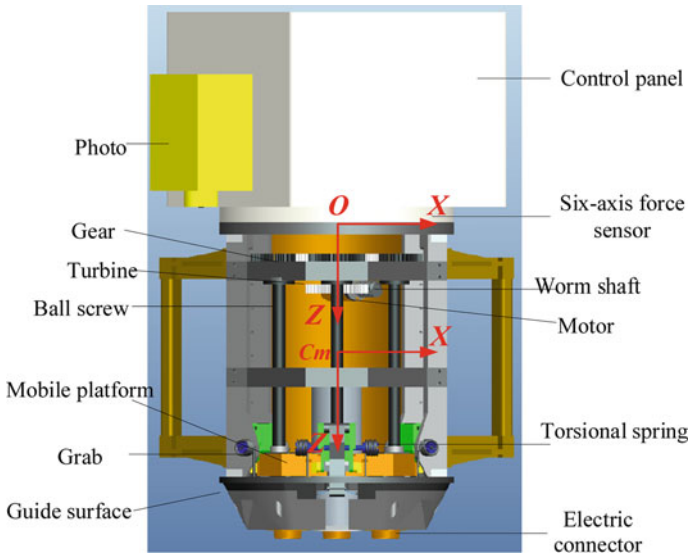
Fig. 4 Dynamic model of the end-effector

of the mobile platform, closure and the rigid connection between the adapter and end-effector can be implemented by the grab mechanism.

Based on the established model as mentioned above, the model of the space manipulator system can be built. As shown in Fig. 5, there are four main parts in the space manipulator system, which include the cabin, the manipulator, the end-effector and the adapter. Practically, the space manipulator is consisted of 7 flexible joint and 2 arm links. The end-effector and the adapter are respectively fixed on the output shaft of the 7th joint and the cabin. In the next section, it will be expounded about docking and capturing process.

4 Dynamic Behaviour Analysis in the Docking and Capturing Process

In this section, a numerical method about the docking and capturing process is firstly presented. By adopted the numerical results, effects of joint stiffness and the flexibility of arm links on the dynamic behaviour of the space manipulator are demonstrated.

Fig. 5 Dynamic model of
the space manipulator system
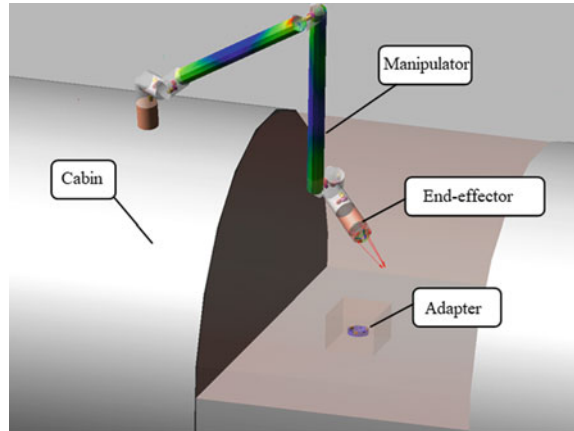
4.1 Numerical Method About the Docking and Capturing Process

As a typical and frequent task, shifting the load module by using the space manipulator is selected to analyze its dynamic behaviour and force-closure properties. Based on the model built in Sect. 3, path planning of the shifting load module is shown in Fig. 6. Corresponding with the practical working conditions, the end of manipulator is at mb1 point at the initial state and will arrive at the docking position with the predefined speed v1 = 0.15°/s, which is defined preparing stage. From mb2 to mb3, docking and capturing process is accomplished, which is defined capturing stage. It should be noted the strategy of joints speed applies the trapezoidal planning.

And the corresponding angular displacement of joints is depicted in Table 2. Notably, the first joint θ_1 is fixed at 90°. Moreover, it should be noted the load of the task is 1000 kg. The quality for the core cabin, test cabin I and test cabin II are same, which are 2.2×104 kg. Besides, the stiffness of harmonic reducer and torque

Fig. 6 Path planning of the
shifting the load module
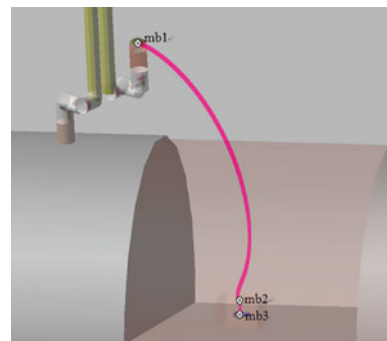
sensor is 2094 Nm/° and 8484 Nm/°, respectively. Also, T700/Ag-80 is selected as the material of arm links.

In the docking and capturing process, the end location error could lead to the force-closure phenomenon. In this paper, 1 mm represented the end location error between the end-effector operation target and the adapter is adopted to analyse the dynamic behaviour and force-closure properties.

4.2 Effect of Joints Stiffness on the Dynamic Behaviour

Considering the joints stiffness is a key parameter to affect the dynamic behaviour of space manipulator system, the contact force at the docking and capturing guide interface, the maximum joint torque and angle error are computed and depicted in Fig. 7. High joints stiffness represented as 10 times of designed joints stiffness is adopted to demonstrate effects of joints stiffness. It can be found the space manipulator system is at preparing stage before $t \approx 80$ s and then arrives at the capturing stage. Meanwhile, from Fig. 7a, it can be seen the maximum contact force at the guide interface between the end-effector and the adapter for high joints stiffness is 168.3 N, which is higher compared to that for designed joints stiffness. Besides, the load torque for the space manipulator system with higher joints stiffness is more heavy. However, it can be observed that the higher joints stiffness will result to smaller joint error. Conclusions can be obtained the contact force and load torque in docking and capturing process is higher with increasing the joints stiffness.

4.3 Effect of Manipulator Flexibility on the Dynamic Behaviour

Similar to the study mentioned, Fig. 8 shows the effect of the manipulator flexibility on the dynamic behaviour for the space manipulator system. It can be seen the maximum contact force at the guide interface between the end-effector and the adapter is 28.3 N when the manipulator flexibility is regarded, which is higher compared to that without the manipulator flexibility. Also, similar regular is observed for the load torque. Moreover, the manipulator flexibility will lead to smaller joint error. Namely, when the manipulator flexibility is introduced, the maximum contact force at the guide interface between the end-effector and the adapter, the load torque and the joint error are lower.

Fig. 7 Dynamic behaviour of space manipulator system with different joints stiffness **a** contact force at the guide interface **b** load torque of partial enlargement **c** angle error of partial enlargement
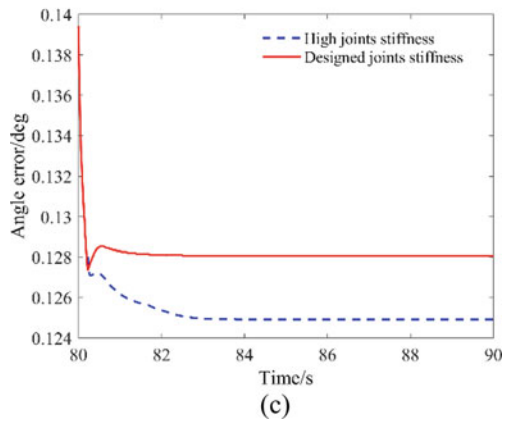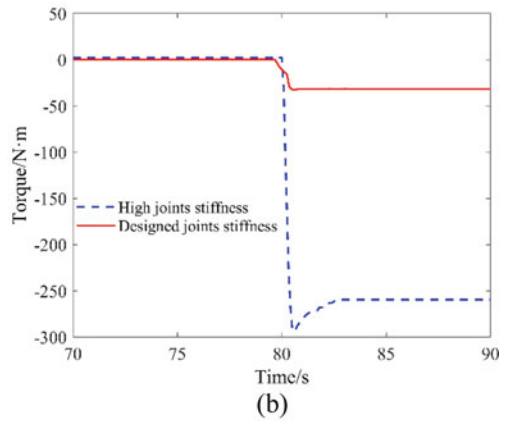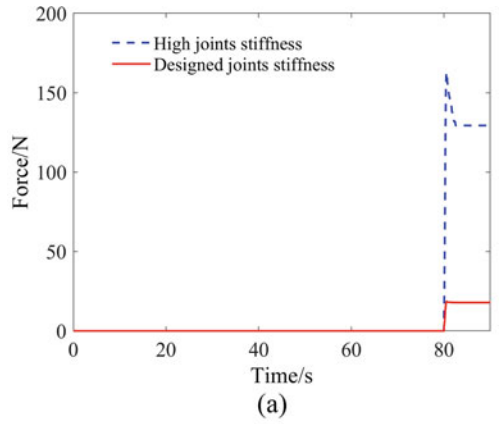

(a)

(b)

(c)

Fig. 8 Dynamic behaviour of space manipulator system with different manipulator flexibility **a** contact force at the guide interface **b** load torque of partial enlargement **c** angle error of partial enlargement
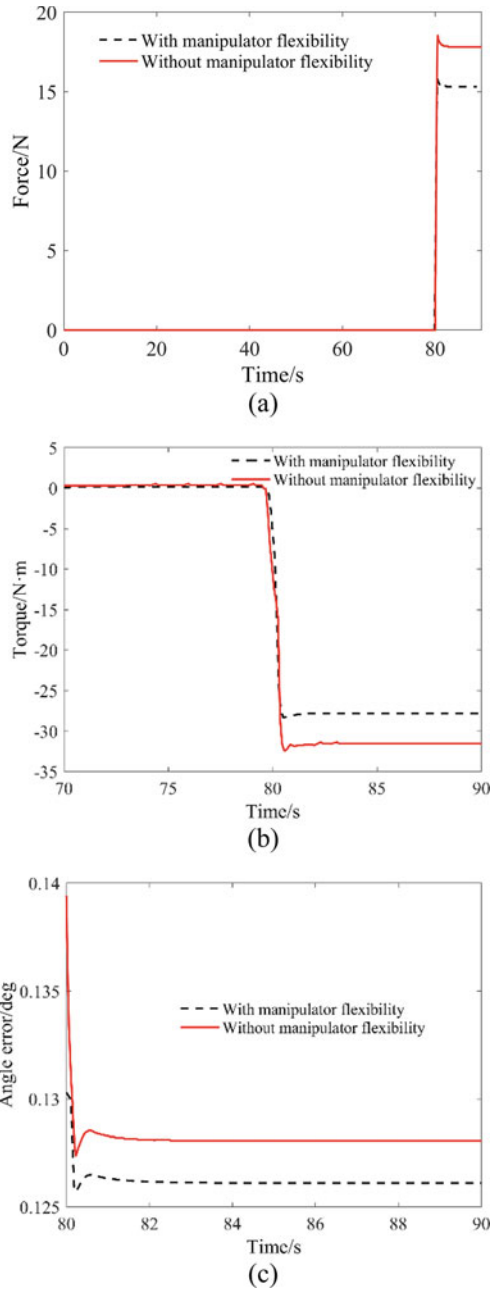

(a)

(b)

(c)

5   Conclusions

In this paper, a parametric modelling method for the flexible space manipulator system was presented and a rigid-flexible dynamic model for the space manipulator applying in the space station was developed. Kinematic structure analysis, dynamic behaviour analysis, and force-closure properties analysis during docking and capturing process have been conducted to evaluate the manipulator flexibility and joints stiffness. Based upon these results, conclusions can be obtained:

(1). The parametric modelling method and the rigid-flexible dynamic model for the space manipulator applying in the space station proposed in this paper work well for investigating the dynamic behaviour during docking and capturing process.

(2). The maximum contact force at the guide interface between the end-effector and the adapter, the load torque decreases with the increase of joints stiffness. Similar change law is presented when the manipulator flexibility is considered. However, the joint error decreases with the increase of joints stiffness or the introduction of the manipulator flexibility.

In fact, the rigid-flexible dynamic model developed in this paper can simulate many other working processes such as plugging. Besides, as the rigid-flexible dynamic model considering many actual complex attached institutions, the parametric modelling method and results in this paper can help researcher have a better understanding of structure design and application for the space manipulator.

References

1. Moghaddam B, Chhabra R (2021) On the guidance, navigation and control of in-orbit space robotic missions: a survey and prospective vision. Acta Astronaut 184:70–100
2. Yonghong M, QunMing L (2009) Analysis of gripping contact force and force-closure of manipulator. J Central South Univ (Sci Technol) 40(6):1580–1586
3. Fan M, Tang L (2021) Impact analysis and trajectory planning stabilization control for space robot after capturing target. J Astronaut 42(10):1305–1316
4. Salvioli F, Capasso F, Ferrentino E, Pasqualeb C (2022) Globally-optimal whole body motion planning under nonholonomic constraints using dynamic programming. Acta Astronaut 193:619–626
5. Shi C, Guo H et al (2021) Design and assembly performance analysis of large space structure assembly interface. J Astronaut 42(12):1493–1501
6. Jiang W, Shi Y et al (2022) Research on mechanism configuration and dynamic characteristics for multi-split transmission line mobile robot. Ind Robot 49(2):200–211
7. Chen N, Zhang Y, Cheng W (2021) Space detumbling robot arm deployment path planning based on Bi-FMT* algorithm. Micromachines 12(10):1231

8. Du Y, Wang C (2020) Dynamic coupling and control of flexible space robots. Int J Struct Stab Dyn 20(9):2050103
9. Kang G, Zhang Q et al (2020) Pd-impedance combined control strategy for capture operations using a 3-dof space manipulator with a compliant end-effector. Sensors 20(23):1–22
10. Sun D, Zhang B, Liang X, Shi Y, Suo B (2019) Dynamic analysis of a simplified flexible manipulator with interval joint clearances and random material properties. Nonlinear Dyn 98:1049–1063
11. Liu Y, Jiang D et al (2022) Grasping posture of humanoid manipulator based on target shape analysis and force closure. Alex Eng J 61(5):3959–3969
12. Li J, Huang H, Yan S, Yang Y (2021) Kinematic accuracy and dynamic performance of a simple planar space deployable mechanism with joint clearance considering parameter uncertainty. Acta Astronaut 136:34–45
13. Carabis D, Wen J (2018) Slip avoidance in dual-arm manipulation. In: IEEE international conference on intelligent robots and systems, Madrid, Spain, October 1–5, 2872–2879
14. Ouyang B, Shang W (2015) A new computation method for the force-closure workspace of cable-driven parallel manipulators. Robotica 33(3):537–547
15. Shinde P, Sen S, Shome S (2017) Task space stiffness analysis of wire driven parallel manipulator. In: 2017 1st international conference on electronics, materials engineering and nano-technology, IEMENTech, Science City, Kolkata, 2017, April 28–29, 8077014
16. Yan L, Mu Z, Xu W (2014) Analytical inverse kinematics of a class of redundant manipulator based on dual arm-angle parameterization. In: Proceedings of the IEEE international conference on systems, man, and cybernetics, pp 3744–3749